Catal Lett (2014) 144:1164–1169
DOI 10.1007/s10562-014-1274-9

Probing the Catalytic Function of External Acid Sites Located on the MFI Nanosheet for Conversion of Methanol to Hydrocarbons

Wookdong Kim · Ryong Ryoo

Received: 7 April 2014 / Accepted: 12 May 2014 / Published online: 25 May 2014

Abstract The surfactant-directed MFI zeolite nanosheet of 2.5-nm thickness has been re-investigated to clarify whether the catalytic function in the methanol-to-hydrocarbon (MTH) reaction originates from acid sites located solely in the internal micropores or also on the external surfaces. Two catalytic reactions were measured after all acid sites on the external surfaces were poisoned with triphenylphospine oxide. One reaction was the catalytic cracking of triisopropylbenzene, which can occur only on external surfaces. This reaction was completely killed by poisoning. The second reaction was MTH conversion. Unlike the catalytic cracking of triisopropylbenzene, the MTH reaction proceeded at the same rate, even when the external acid sites were poisoned. The result indicated that the MTH reaction occurred inside the internal pores, not at the external surfaces. This information will be useful for understanding MTH catalysis of other hierarchical zeolites.

Keywords Methanol to hydrocarbon · Zeolite catalyst · External acid sites · Hierarchical zeolite · MFI zeolite nanosheet · ^{31}P NMR

Electronic supplementary material The online version of this article (doi:10.1007/s10562-014-1274-9) contains supplementary material, which is available to authorized users.

W. Kim · R. Ryoo (✉)
Department of Chemistry, KAIST, Daejeon 305-701, Korea
e-mail: rryoo@kaist.ac.kr

W. Kim · R. Ryoo
Center for Nanomaterials and Chemical Reactions, Institute for Basic Science (IBS), Daejeon 305-701, Korea

1 Introduction

Methanol can be produced via syngas from natural gas [1–5]. The production costs of methanol are expected to decrease with the recent development of shale gas (natural gas trapped in shale formations) extraction, which has brought about a renewed interest in the conversion of methanol to hydrocarbons (MTH). Zeolites are known as the most suitable catalyst for the MTH reaction due to the strongly acidic sites present on the zeolite frameworks. According to the hydrocarbon pool mechanism, organic molecules (so-called hydrocarbon pool species) are initially produced from a small amount of methanol at the acid sites. The organic molecules accumulate to form a hydrocarbon pool within the zeolite pores possessing strongly acidic sites. The hydrocarbon pool acts as a co-catalyst to convert more methanol to hydrocarbons [6–8]. A side reaction is the unwanted conversion of the hydrocarbon pool species to polycyclic aromatic hydrocarbons (PAHs) or coke that causes the catalytic deactivation [9, 10]. Among zeolites, the zeolite with MFI topology is known as the most efficient catalyst exhibiting high catalytic activity and long lifetime [2]. The aluminosilicate form of MFI zeolite is known to possess strong Brønsted acid sites. Moreover, the framework of the MFI zeolite is composed of a 3-dimensional (3D) interconnection of straight channels of a 0.54 × 0.56 nm cross section and sinusoidal channels of 0.53 × 0.55 nm. The 3D pore system with the pore cross sections and strongly acidic sites are well suited to form catalytically active hydrocarbon pool species, without the rapid formation of bulky PAHs [2].

Choi et al. [11] reported that the MFI zeolite nanosheet of 2.5 nm thickness exhibited more than 5-times longer catalytic lifetime in the MTH reaction than conventional

MFI zeolite. They attributed the catalytic longevity to facile diffusion of coke precursors from the micropores to outside, assuming that the catalytic reaction would occur in the micropores [11, 12]. More recent investigations revealed that the MFI zeolite nanosheet possessed strongly acidic sites on the external surfaces (i.e., external acid sites), as well as in the internal micropores. The external acid sites exhibited high catalytic activity and long lifetime for hydrocarbon cracking and Friedel–Crafts alkylation reactions [13–15]. Therefore, the strong external acid sites might have also caused the MTH catalytic reactions. Considering this point, we re-investigated the MTH reaction, focusing on the external acid sites on the MFI zeolite nanosheet. We prepared a series of MFI zeolite samples having different external surface areas, by controlling the framework thickness. We measured the catalytic activity after deactivating the external acid sites of the MFI zeolite nanosheet to measure the contribution of external acid sites. The deactivation was conducted by irreversible chemisorption of a bulky basic molecule, i.e., triphenylphosphine oxide, onto the external acid sites.

2 Experimental Section

2.1 Preparation and Characterization of MFI Zeolites

Three samples of MFI zeolite were obtained following the synthesis procedures described elsewhere [16]. These samples are designated as 'NS-2.5', 'NC-20' and 'B-300'. The NS-2.5 sample was the 2.5-nm nanosheet MFI zeolite which was synthesized using $C_{16}H_{33}$–$N^+(CH_3)_2$–C_6H_{12}–$N^+(CH_3)_2$–C_6H_{13} as a structure-directing-agent (SDA). The NC-20 sample was a nanocrystalline MFI zeolite exhibiting a mode particle diameter at 20 nm along the shortest axis, and synthesized using C_3H_7–$N^+(CH_3)_2$–C_6H_{12}–$N^+(CH_3)_2$–C_3H_7 as the SDA. The B-300 sample was a bulk zeolite exhibiting a mode crystal diameter of 300 nm. This sample was synthesized using tetrapropylammonium bromide as an SDA. The details of the synthesis procedures were the same as described in Ref. 16, except that the synthesis temperature for NC-20 was changed to 423 K to increase the particle diameter. The samples were characterized using powder X-ray diffraction (XRD, Rigaku Multiflex diffractometer), N_2 adsorption–desorption (Micromeritics TriStar-II volumetric adsorption analyzer), scanning electron microscopy (SEM, FEI Verios 460L), and transmission electron microscopy (TEM, Tecnai G2 F30). All characterizations were carried out following the same procedures described in the literature [16], except for the difference in the SEM instruments. The concentration of Brønsted acid sites were quantitatively analyzed using chemisorption of phosphine oxides. The chemisorption was detected by ^{31}P NMR spectroscopy (Bruker AVANCE400WB spectrometer) with respect to the location of acid sites (i.e., total versus external acid sites), following the method in the literature [14].

2.2 MTH Reaction

The MTH reaction was carried out in a fixed-bed, fused quartz reactor (inner diameter = 11 mm) under atmospheric pressure. For the reaction measurement, zeolite catalyst (0.10 g) was diluted with silicon carbide (1.0 g) to dissipate the heat of reaction. Prior to the measurement, the catalyst was activated under a dry nitrogen flow at 673 K. To this catalyst bed, methanol vapor saturated in a nitrogen flow was supplied. The methanol saturation was performed by using a bubble saturator at the nitrogen flow rate of 40 mL min^{-1} at 293 K. The weight hourly space velocity (WHSV) of methanol was evaluated as 4.5 h^{-1}, with the assumption of complete methanol saturation in the nitrogen flow. The MTH reaction was performed over the temperature range of 523–653 K. The reaction temperature was measured by a K-type thermocouple inserted in the reactor through a thermocouple well. The reactor effluent was analyzed by a gas chromatograph (GC, Younglin Acme-6000) equipped with a flame-ionization detector (FID). A HP-Plot Q capillary column (30 m × 0.53 mm × 40 μm, J&W) was used for an accurate analysis of the catalytic conversion.

2.3 Deactivation of External Acid Sites and Cracking of 1,3,5-Triisopropylbenzene

All the external acid sites of the MFI zeolite nanosheet were deactivated by the chemisorption of triphenylphosphine oxide (TPPO). Before the adsorption of TPPO, a sample of the MFI nanosheet (1.0 g) was fully dehydrated under vacuum at 573 K. The dehydrated zeolite was added into a methylene chloride solution containing TPPO (0.030 g). Subsequently, the methylene chloride solvent was removed by evacuation at room temperature. To measure the catalytic cracking of 1,3,5-triisopropylbenzene, zeolite catalyst (0.020 g) was placed in a fixed bed stainless-steel reactor (inner diameter = 4 mm). Prior to the reaction measurement, the catalyst in the reactor was heated to 573 K for 2 h under nitrogen flow at 20 mL min^{-1}. Subsequently, 1,3,5-triisopropylbenzene (TIPB, 95 %, Sigma-Aldrich) was fed through a syringe pump (KD Scientific) at the feeding rate of 0.20 mL h^{-1} (WHSV of TIPB = 8.5 h^{-1}, and N_2/TIPB molar ratio = 50). The reaction effluent was analyzed using an online GC (Younglin, Acme-6000) equipped with a FID. The products were separated by a GS-GasPro capillary column (30 m × 0.32 mm, J&W).

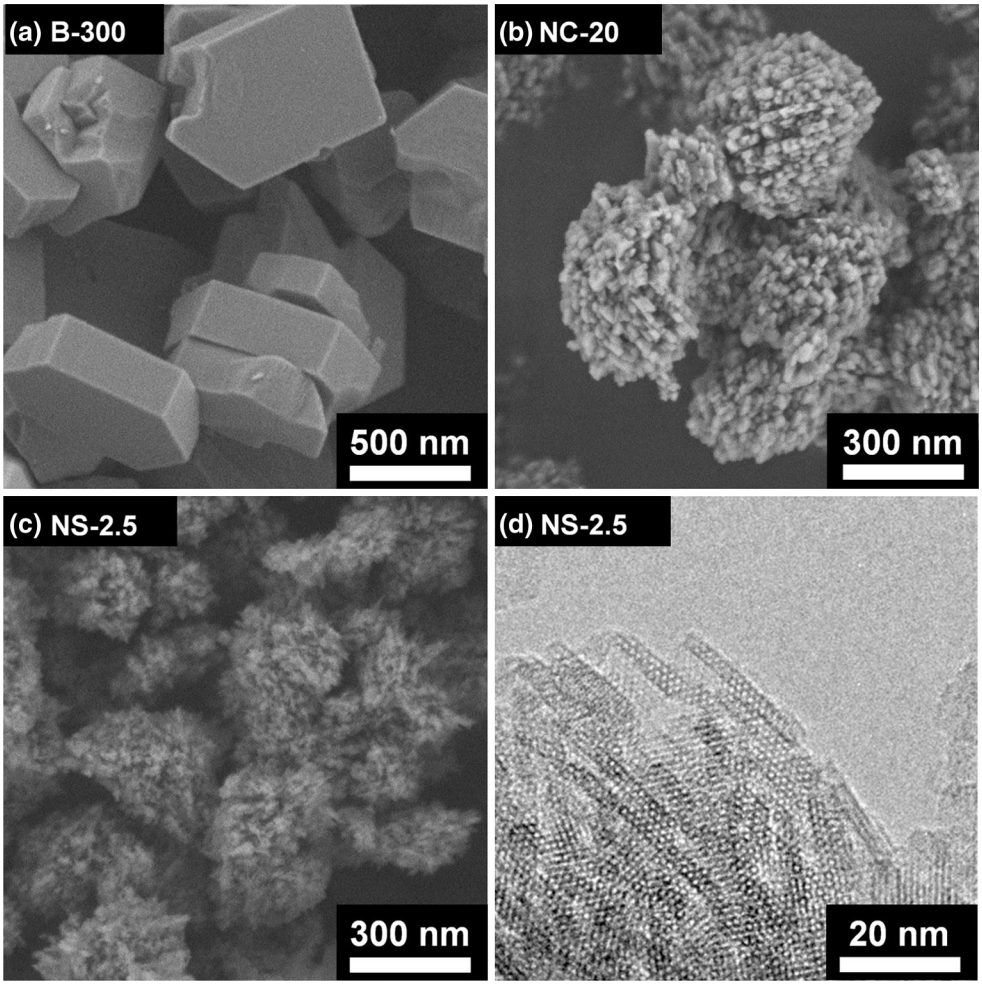

Fig. 1 Representative SEM images of **a** B-300, **b** NC-20, **c** NS-2.5 zeolite samples, and **d** TEM image of NS-2.5

3 Results and Discussion

3.1 Zeolite Catalyst with Various Crystal Thicknesses

Figure 1 shows the representative SEM and TEM images of the three MFI zeolite samples (NS-2.5, NC-20 and B-300) investigated in the present work. These images were used to determine the mode values of the zeolite particle diameters (i.e., 2.5 nm for NS-2.5, 20 nm for NC-20, and 300 nm for B-300). The MFI structure of the samples was confirmed by the XRD patterns shown in Fig. 2a. The porous textural properties of these samples were evaluated from the N_2 isotherm data shown in Fig. 2b. The properties are summarized in Table 1. The specific surface area (Table 1) was calculated by the Brunauer–Emmett–Teller (BET) equation. The external surface area was estimated using the *t*-plot method. Both the specific surface area and the external surface area of the zeolite samples increased as the crystal thickness decreased. For example, the NS-2.5 sample exhibited an external surface area of 350 $m^2\ g^{-1}$, a value six-times larger than that for B-300 (60 $m^2\ g^{-1}$).

The Si/Al ratios of the zeolite samples were determined by elemental analysis using inductively coupled plasma emission. The analytical results (Table 1) show that all the zeolite samples synthesized in this work had very similar Si/Al ratios (48 ± 2). The Brønsted acid sites originating from the Al incorporation were quantitatively analyzed with respect to their locations, using the chemisorption of phosphine oxides. Trimethylphosphine oxide (TMPO) was used for the detection of the total amount of strong Brønsted acid sites (external surfaces plus internal pores). Tributylphosphine oxide (TBPO) was used to determine the external acid sites since the bulky molecules can probe only the external acid sites without entering the micropores. A magic angle spinning ^{31}P NMR spectrum was recorded successively after each of the phosphine oxides was fully dosed onto each sample. The ^{31}P NMR chemical shifts were used to distinguish strongly acidic sites from weak acid sites. The amounts of the strongly acidic sites

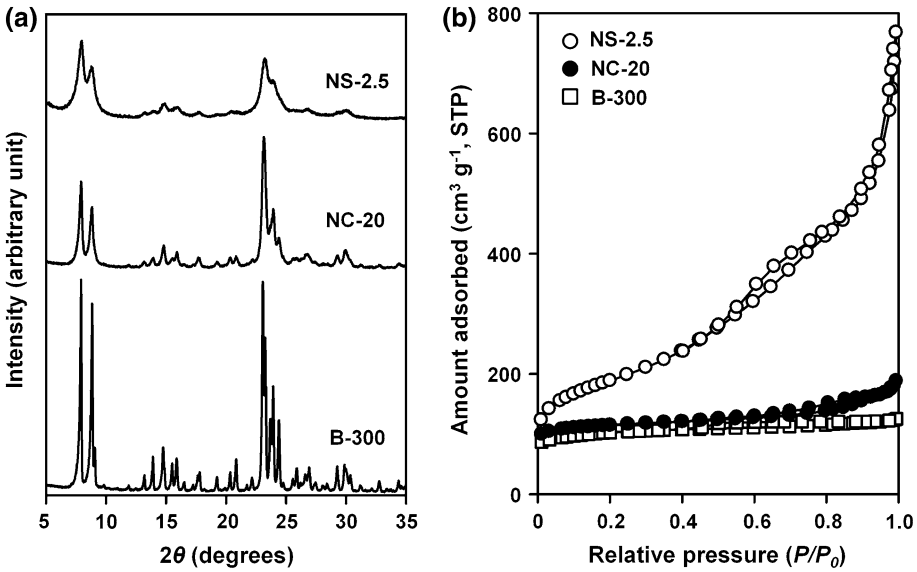

Fig. 2 **a** Powder XRD patterns and **b** N_2 adsorption–desorption isotherms (measured at 77 K) of NS-2.5, NC-20 and B-300 zeolite samples

Table 1 Physicochemical properties of MFI zeolite samples investigated as catalyst

Samples	Si/Al[a]	S^{b}_{BET} (m^2 g^{-1})	S^{c}_{ext} (m^2 g^{-1})	BA^{d}_{tot} (μmol g^{-1})	BA^{e}_{ext} (μmol g^{-1})	BA_{ex}/BA_{tot} (%)
B-300	46	380	60	190	8	4
NC-20	50	440	120	180	22	12
NS-2.5	48	600	350	160	45	28

[a] Molar ratio by elemental analysis using inductively coupled plasma emission (Optima 4300 DV, Perkin-Elmer)

[b] BET surface area from N_2 adsorption in the relative pressure range of 0.05–0.20

[c] External surface area according to the *t*-plot method

[d] Concentration of total Brønsted acid sites

[e] Concentration of external Brønsted acid sites

were determined from the intensities of the NMR signals (see Fig. S1 in Supporting Information for the NMR spectra, and Ref. 14 for the detailed analytical procedure). The concentration of the strongly acidic sites obtained in this manner for each sample (Table 1) showed that the total acid concentration was very similar for all the zeolite samples investigated here. These values were in good agreement with their similarity in Si/Al ratios. On the other hand, the external acid concentration changed in the order of B-300 < NC-20 < NS-2.5, which was consistent with the increasing order of the external surface areas. Note that the NS-2.5 sample contained 45 μmol g^{-1} of external acid sites. This value corresponded to 28 % of the total strong acid concentration. In the case of B-300, only 4 % of the total acid sites (8 μmol g^{-1}) were located at the external surface.

3.2 MTH Reactions Over MFI Zeolites

In Fig. 3, the hydrocarbon yields in the MTH reaction were plotted against the catalytic reaction time on stream at each temperature. Dimethyl ether (DME) was present in the product stream as a result of the methanol dehydration reaction [1, 2]. The DME production was not included in the hydrocarbon yields, according to the convention on MTH analysis [16]. In the case of the B-300 catalyst at 553 K, the conversion-*vs*.-time plot in Fig. 3a showed an initial induction period for about 2 h before reaching the full conversion value of approximately 25 %. The induction period can be explained by the hydrocarbon pool mechanism [1, 2, 5]. In this mechanism, the MTH catalytic activity of a zeolite is known to increase during the induction period as the catalytically active hydrocarbon pool species are gradually built up on the surface of the zeolite framework. The concentration of the hydrocarbon pool species reaches a steady state with time, whereas the accumulation rate is balanced with the rate of diffusion to outside. The MTH conversion stops increasing further once the steady state is reached. Subsequently, the catalytic conversion rate decreases rather gradually over a long period of time. This decrease is attributed to the catalyst deactivation due to coke deposition. Thus, the catalytic conversion plot showed a maximum point shortly after the induction period. The duration of the induction period for B-300 decreased very fast as the reaction temperature increased to 573 K (Fig. 3). Therefore, at 583 K, the catalyst exhibited the full MTH conversion without a distinct induction period.

In the present context, we have defined the 'catalytic activity' of a catalyst as the hydrocarbon yield (wt%) attainable at the maximum point following the induction

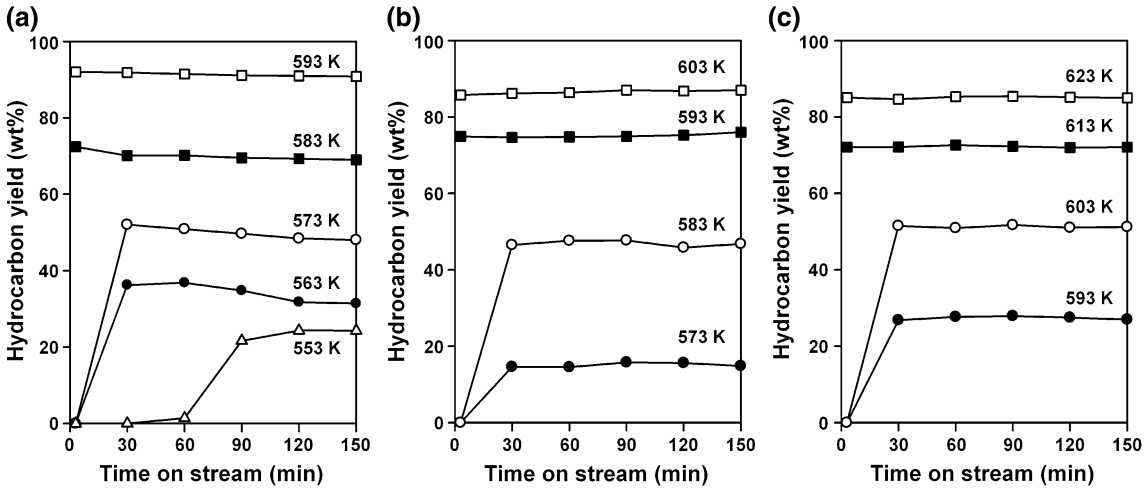

Fig. 3 The hydrocarbon yield in MTH reaction using **a** B-300, **b** NC-20, and **c** NS-2.5 zeolites as catalysts was plotted as a function of time on stream (Reaction condition: mass of catalyst = 0.10 g, and WHSV of methanol = 4.5 h^{-1})

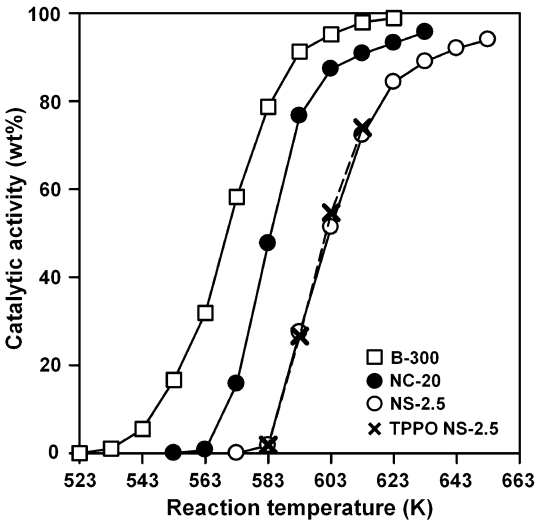

Fig. 4 The maximum hydrocarbon yield, which was obtained shortly after the induction period in Fig. 3, was plotted as a function of reaction temperature. The 'X'-marked data points were obtained from NS-2.5 after poisoning all the external acid sites with TPPO

period (Fig. 3). The catalytic activity defined in this manner was plotted as a function of the reaction temperature in Fig. 4. Each zeolite catalyst in Fig. 4 exhibited an S-shape curve. The position of each S-curve was shifted to the high temperature side by approximately 20 K in the order of B-300 < NC-20 < NS-2.5. The catalytic activity of B-300 was 1 % at 523 K, and increased steeply with temperature to reach 91 % at 593 K. The NC-20 catalyst exhibited a detectable conversion at 563 K, while NS-2.5 became active at 583 K. Thus, the catalytic activity decreased in the order of decreasing crystal thickness: B-300 > NC-20 > NS-2.5.

3.3 Effect of Surface Poisoning on MTH Reaction

The 'X'-marked' data points in Fig. 4 were obtained from the MTH reaction performed with the NS-2.5 catalyst after all the external acid sites on this sample were completely poisoned with TPPO. Note that TPPO was selected in the present study as a strong base that would neutralize the strong Brønsted acid sites in a zeolite. Furthermore, TPPO was assumed to be too bulky to enter the 10-membered ring micropore openings in the MFI zeolite structure. The mouth of each pore of the straight channels in the zeolite was 0.54 × 0.56 nm in cross section while the sinusoidal channels were 0.53 × 0.55 nm. Neither of the channels was assumed as accessible for TPPO molecules whereas the molecular diameter of TPPO (~1.17 nm) would be much larger than the zeolite pore apertures. With these assumptions, TPPO was used to poison selectively the Brønsted acid sites present on the external surfaces of NS-2.5 [17]. These assumptions were checked using the catalytic cracking of 1,3,5-triisopropylbenzene (TIPB). This reaction is known to occur only at the external surface, due to the molecular diameter exceeding the size of the MFI pore mouths [18, 19]. As the reaction data is provided in Fig. S2, the pristine NS-2.5 zeolite exhibited a TIPB conversion of 15 % at 573 K. The TIPB conversion dropped to zero after poisoning with TPPO. The TIPB conversion was measured parallel (i.e., not consecutively) to the MTH reaction at 573 K, using separate aliquots taken from the same batch of TPPO-poisoned catalyst sample.

For the MTH reaction temperatures above 573 K, the TPPO-poisoning effect was further checked in the following manner: TIPB cracking of the TPPO-poisoned NS-2.5 zeolite was consecutively measured on exactly the same sample after each run of MTH reaction to obtain an

'X'-marked' data point in Fig. 4. The TPPO-treated nanosheet was still totally inactive for the TIPB cracking reaction over the temperature range of 583–613 K. However, when the reaction temperature was exceedingly increased to 623 K or higher, the poisoned catalyst partially regained the TIPB cracking activity. This result indicated that the initially chemisorbed TPPO was desorbed or decomposed during the MTH reaction to 623 K or higher temperatures. In this regard, the catalytic result of the MTH reaction was compared between the 'X'- and 'O'-marked data points (Fig. 4) within the limited range of 583–613 K. Nevertheless, the experiment was sufficient to investigate the TPPO poisoning effect on the MTH conversion. Furthermore, the whole process of 'TPPO poisoning'–'MTH reaction'–'TIPB cracking' was checked a total of three times using three aliquots of NS-2.5, and the same result was reproducible within the error range of ±2 % in MTH conversion.

As judged from the 'X'- and 'O'-marked data points in Fig. 4, the MTH reaction was not altered at all by the external surface poisoning with TPPO. That is, the Brønsted acid sites present on the external surfaces played a negligible role in the MTH reaction. Due to insignificant catalytic function of the external acid sites, it could be inferred that the MTH reaction occurred mostly at the internal acid sites of the MFI zeolites. The concentration of the internal acid sites can be calculated by subtracting the concentration of the external acid sites from that of the total acid sites. According to this calculation, the NS-2.5 sample had the internal acid concentration of 115 μmol g^{-1} while B-300 had 182 μmol g^{-1}. As compared to the bulk zeolite, the low catalytic conversion of the MFI nanosheet (Fig. 3) can be attributed to the low concentration of the internal acid sites. However, the catalytic conversion of the MFI nanosheet at low temperature (<583 K) was too low to explain the result by the low concentration of the internal acid sites. For instance, the NS-2.5 catalyst exhibited only a 1 % MTH conversion at 583 K, while the B-300 showed 75 %. Perhaps the internal acid sites of the nanosheet are less active than those of bulk zeolite, for reactions involving hydrocarbons [20]. Bleken et al. [21] speculated that such a low catalytic activity of the MFI nanosheet could be due to the rapid diffusion of the hydrocarbon pool species toward the outside, so that the diffusion would decrease the concentration of hydrocarbon pool species inside the micropore channels.

4 Conclusion

The MFI zeolite nanosheet studied in this investigation was only 2.5 nm in thickness. For such a thin zeolite nanosheet, approximately 60 % of the total BET surface area corresponded to the external surfaces. The external surfaces contained approximately 30 % of all the Brønsted acid sites present in the zeolite nanosheet. Among the external acid sites, there were plenty of strongly acidic sites that could catalyze the hydrocarbon cracking reactions and Friedel–Crafts alkylation. Despite the presence of the strongly acidic sites, the external surface of the MFI nanosheet did not catalyze the methanol-to-hydrocarbon reaction, as confirmed by the surface poisoning effects of triphenylphosphine oxide. Hence, we concluded that the methanol-to-hydrocarbon reaction occurred solely inside the micropores of the MFI zeolite. This result is consistent with the hydrocarbon pool mechanism in which pores of appropriate diameters are necessary for the formation of hydrocarbon pools. The present information may be extended to other hierarchically porous MFI zeolites that can be prepared by various synthetic or post-synthetic routes developed in recent years.

Acknowledgments This work was supported by Institute for Basic Science (IBS) [CA1401].

References

1. Stöcker M (1999) Microporous Mesoporous Mater 29:3
2. Olsbye U, Svelle S, Bjørgen M, Beato P, Janssens TVW, Joensen F, Bordiga S, Lillerud KP (2012) Angew Chem Int Ed 51:5810
3. Teketel S, Svelle S, Lillerud KP, Olsbye U (2009) ChemCatChem 1:78
4. Teketel S, Skistad W, Benard S, Olsbye U, Lillerud KP, Beato P, Svelle S (2012) ACS Catal 2:26
5. Haw JF, Song W, Marcus DM, Nicholas JB (2003) Acc Chem Res 36:317
6. Dahl IM, Kolboe S (1993) Catal Lett 20:329
7. Dahl IM, Kolboe S (1996) J Catal 161:304
8. Svelle S, Joensen F, Nerlov J, Olsbye U, Lillerud KP, Kolboe S, Bjørgen M (2006) J Am Chem Soc 128:14770
9. Fu H, Song W, Haw JF (2001) Catal Lett 76:89
10. Schulz H (2010) Catal Today 154:183
11. Choi M, Na K, Kim J, Sakamoto Y, Terasaki O, Ryoo R (2009) Nature 461:246
12. Kim J, Choi M, Ryoo R (2010) J Catal 269:219
13. Shetti VN, Kim J, Srivastava R, Choi M, Ryoo R (2008) J Catal 254:296
14. Seo Y, Cho K, Jung Y, Ryoo R (2013) ACS Catal 3:713
15. Kim JC, Cho K, Ryoo R (2014) Appl Catal A 470:420
16. Kim J, Kim W, Seo Y, Kim JC, Ryoo R (2013) J Catal 301:187
17. Chen CSH, Schramm SE (1996) Microporous Mater 7:125
18. Hibino T, Niwa M, Murakami Y (1991) J Catal 128:551
19. Kim JH, Ishida A, Okajima M, Niwa M (1996) J Catal 161:387
20. Verheyen E, Jo C, Kurttepeli M, Vanbutsele G, Gobechiya E, Korányi TI, Bals S, Tendeloo GV, Ryoo R, Kirschhock CEA, Martens JA (2013) J Catal 300:70
21. Bleken BTL, Wragg DS, Arstad B, Gunnæs AE, Mouzon J, Helveg S, Lundegaard LF, Beato P, Bordiga S, Olsbye U, Svelle S, Lillerud KP (2013) Top Catal 56:558